LA-UR-14-20246
Approved for public release; distribution is unlimited.

Title: Efficient Algorithm for Locating and Sizing Series Compensation Devices in Large Transmission Grids: Solutions and Applications (PART II)

Author(s): Frolov, Vladimir
Backhaus, Scott N.
Chertkov, Michael

Intended for: arXiv
IEEE Power Systems

Issued: 2014-01-14

Efficient Algorithm for Locating and Sizing Series Compensation Devices in Large Transmission Grids: Solutions and Applications

Vladimir Frolov[(1,4)], **Scott Backhaus** [(2,4)] and **Misha Chertkov** [(3,4,1)]
[(1)] Moscow Institute of Physics and Technology, Dolgoprudnyj, Moscow Region, 141700, Russia
& Skolkovo Institute of Science and Technology, Skolkovo 143025, Russia
[(2)] Material Physics and Applications Division, LANL, Los Alamos, NM 87545, USA
[(3)] Center for Nonlinear Studies and Theoretical Division, LANL, Los Alamos, NM 87545, USA
[(4)] New Mexico Consortium, Los Alamos, NM 87544, USA

***Abstract*—In a companion manuscript [1], we developed a novel optimization method for placement, sizing, and operation of Flexible Alternating Current Transmission System (FACTS) devices to relieve transmission network congestion. Specifically, we addressed FACTS that provide Series Compensation (SC) via modification of line inductance. In this manuscript, this heuristic algorithm and its solutions are explored on a number of test cases: a 30-bus test network and a realistically-sized model of the Polish grid ($\sim$ 2700 nodes and $\sim$ 3300 lines). The results on the 30-bus network are used to study the general properties of the solutions including non-locality and sparsity. The Polish grid is used as a demonstration of the computational efficiency of the heuristics that leverages sequential linearization of power flow constraints and cutting plane methods that take advantage of the sparse nature of the SC placement solutions. Using these approaches, the algorithm is able to solve an instance of Polish grid in tens of seconds. We explore the utility of the algorithm by analyzing transmission networks congested by (a) uniform load growth, (b) multiple overloaded configurations, and (c) sequential generator retirements.**

***Index Terms*—Power Flows, Series Compensation Devices, Non-convex Optimization**

I. Introduction

Flexible Alternating Current Transmission System (FACTS) devices can play several important roles in transmission networks including improving small-signal and transient stability [2], [3], improving voltage regulation [4], [5] and relieving transmission congestion [6]. This paper builds on a number of recent studies that use Series Compensation (SC) devices, a particular type FACTS device, to improve transmission grid operation by modifying transmission line inductance to relieve transmission congestion [7], [8], [9], [10], [11], [12]. In a companion paper [1], we formulated a problem for the optimal placement and sizing of SC devices. In addition, we developed methods that enable efficient solution of the optimization problem to enable consideration SC device placements over large networks. The highlights of our approach from[1] are:

- The use of Sequential Linear Programming (SLP) that linearizes transmission line constraints around the current solution leading to efficient solution of a series of relatively simple Linear Programs (LP).
- The use of an ℓ_1 norm for the cost of SC devices. Even without any explicit incorporation of sparsity, the ℓ_1 norm implicity induces solution sparsity, i.e. only a small number of lines are selected for inductance modification. The selected lines are often not the most severely overloaded line or even overloaded at all.
- The solution sparsity enables efficient solution of the optimization problem via cutting plane methods.

This current manuscript focuses on demonstration of the methods developed in [1] on both test and realistically-sized transmission networks and the analysis of the properties of the results. The cases considered differ in the size of the network and in how the stress is applied to the network to induce congestion.

Our first set of cases utilize a 30-bus network. The simplicity of the network allows us to observe and interpret some general qualitative features of the solutions. Primary among these are a combination of local and non-local effects and sparsity of the solutions. Quite often, our algorithm [1] places SC devices not on the overloaded lines, but on nearby lines, increasing their susceptance to draw power flow away from the overloads. If the overload is too great or if the local network configuration does not allow an entirely non-local solution, the non-local approach is supplemented with the placement of SC devices directly on the overloaded line to reduce its susceptance. Another consistent observation is the sparsity of the optimal SC placements, i.e. we find that very few susceptance modifications are needed to relieve one or a cluster of overloads.

In general, the qualitative features revealed by the 30-bus case studies carry over to a series of case studies on a realistically-sized model of the Polish grid ($\sim$ 2700 nodes and $\sim$ 3300 lines). Our primary motivation for using the Polish grid model is to demonstrate the computational efficiency of our approach developed in Ref. [1]. However, we also use this larger network to explore SC device placement for a range of causes of network stress including uniform load growth, relief of multiple configurations of congestion, and sequential generator retirement.

The remainder of this manuscript is organized as follows. Section II applies our algorithm to the 30-bus model and discusses some of the universal properties of the solutions. Section III applies our algorithm to a model of the Polish grid to demonstrate computational efficiency and interprets the solution structure. Finally, Section IV discusses conclusions and directions for future research.

II. Qualitative Properties of the Solutions: 30-Bus Grid

We first apply our algorithms[1] for placement and sizing of SC devices to a small 30-bus test model available in MatPower[13] (see Fig. 1)[1]. Our intent is to explore the qualitative properties of the solutions generated by our algorithm to build intuition and physical understanding. Later, we demonstrate our algorithms on a much larger, realistically-sized transmission network in Section III, where we utilize the Polish grid ($\sim$ 2700 buses, see Fig. 3) which is also available in Matpower[13].

Before applying our algorithm to the 30-bus network, we first stress the network. Transmission networks can be stressed in a number of different ways, and we explore several on the Polish grid in Section III. However, uniform load growth is simple to apply, and we use it here to explore the properties of solutions reached by our algorithm on the 30-bus network. Starting with a base configuration of load, we solve an DC Optimum Power Flow (DC-OPF) to find the favored configuration of generation. Next we scale both generation and load by the same factor $\alpha > 1$. We increase α until we reach α_c, i.e. the load/generation scale factor that first induces a transmission line overload. We continue to increase α beyond α_c and use our SC placement and sizing algorithm[1] to correct the overloads at minimum cost. We use the ratio α/α_c as a measure of network stress.

For the stressed 30-bus network, our algorithm selected SC device placements with a number of interesting features that we discuss below:

A. Non-locality

The nonlocal influence of SC devices is illustrated on two examples of the 30-node network—the first with $\alpha/\alpha_c = 1.4$ (see Fig. 1) and the second with $\alpha/\alpha_c = 1.9$ (see Fig. 2). In both cases, there were several lines that were overloaded (shown in red) after scaling load and generation by α. We then ran our SC placement and sizing algorithm[1] to correct these overloads. The lines with modified susceptance are marked in green with the adjacent percentages indicating the degree of susceptance modification. For the moderately stressed case ($\alpha/\alpha_c = 1.4$) in Fig. 1, our algorithm chose not to decrease the susceptance of the overloaded (red) lines to restrict the power flow on them. Instead, it modifies the susceptance of nearby lines to reroute power flows around the congested transmission

[1]To convert MatPower cases into the standard format (matrix L and vector p), transformers and phase shifters are turned off, double lines are combined to form one line with value of throughput and inductance calculated from two lines. Double generators also were combined to form one generator.

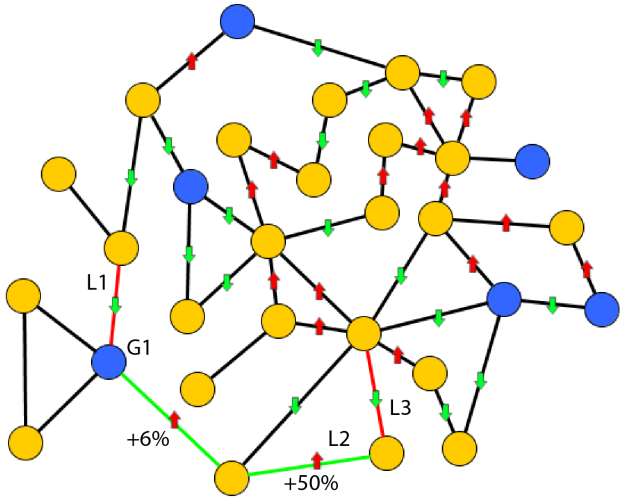

Fig. 1. Visualization of the 30-node model illustrating the non-locality and sparsity of the optimal solution with $\alpha/\alpha_c = 1.40$. The colored nodes indicate loads (yellow) and generators (blue). The two red lines were overloaded in the base case with $\alpha/\alpha_c = 1.4$. The two green lines where selected by our algorithm for susceptance modification by SC devices. The percentage susceptance correction is shown next to the corrected lines. The difference in power flows through the lines after the corrections are shown with short green or red arrows to indicate a decrease or increase of power flow, respectively. If there is no arrow then power flow is nominally the same.

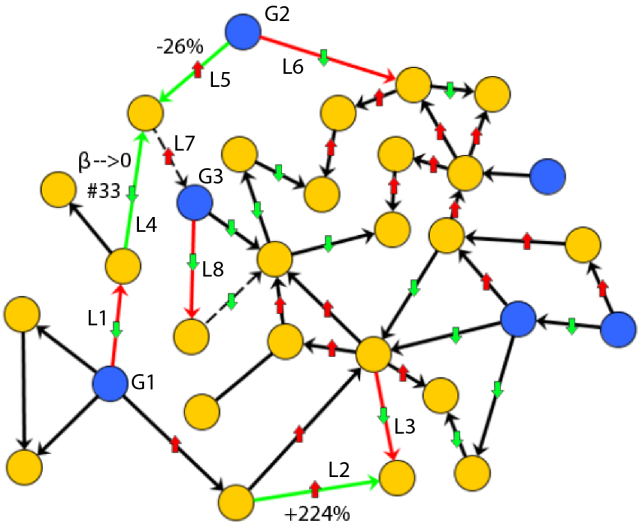

Fig. 2. Same as Fig. 1, but for $\alpha/\alpha_c = 1.90$. Here, four lines were originally overloaded (red), and three lines are modified by SC devices (green). Arrowheads on the transmission lines indicate the direction of the flow prior to the SC corrections. The two dotted transmission lines experienced a reversal of power flow direction after susceptance modification by SC devices. The difference in *magnitude* of the power flows through the lines after the corrections are shown with green or red vertical arrows to indicate a decrease or increase in power flow magnitude, respectively.

lines. In fact, the increase in susceptance of the two green lines in Fig. 1 simultaneously relieves two overloads by encouraging more power flow from generator G1 towards the load node at the end of lines L2 and L3. This modification offsets the flow over the overloaded line L3 and diverts power flow away from overloaded line L1. Nonlocal effects are a general property of

optimal SC solutions suggesting that the optimal placement of SC devices (and FACTS in general) is nontrivial problem and that computationally efficient algorithms (such as the the one we develop in Ref. [1]) will be required for solving realistically-sized networks.

The nonlocal effect of SC devices is apparent again in the severely stressed case ($\alpha/\alpha_c = 1.9$) in Fig. 2. Arrowheads on the lines indicate the direction of the original $\alpha/\alpha_c = 1.9$ power flows and the smaller arrows (green/down or red/up) indicate whether the original power flows are decreased or increased after the SC devices were placed. Similar to the previous case, the original power flows out of generator G1 overloaded line L1. In this instance, our algorithm drives $\beta \to 0$ on line L4 and simultaneously increases β on line L2 effectively cutting G1 off from the upper part of the network and rerouting the power from G1 to the lower right of the network. As in the $\alpha/\alpha_c = 1.4$ case, the increase in power flow on L2 also relieves the overload on L3. This redistribution of power flows from G1 has even longer range effects. The major reduction of flow on line L4 draws more power from G2 (in spite of the decrease in β on L5) relieving the overload on L6. In addition, it forces a reversal of the power flow on line L7 relieving the overload on L8.

In the highly-stressed case (and others cases not shown), we note that our algorithm chose susceptance corrections that set a line's total susceptance to zero, effectively removing the line from the network. We explored this somewhat curious solution by manually removing the line in question (L4 in Fig. 2) and rerunning our algorithm. The resulting solution had approximately the same structure (i.e. same susceptance corrections in the rest of the network) as the original solution where the algorithm automatically drove the susceptance of L4 to zero.

B. Sparsity

Instead of selecting small modifications of many lines throughout the network, our algorithm makes significant susceptance modifications to a only few lines with the number of modified lines typically the same or slightly smaller than the number of overloads in the base case. This solution sparsity is observed in the small 30-bus network in Fig. 1 and Fig. 2 and will also be observed in the much larger Polish network (see Fig. 5). We note that nowhere in our optimization formulation in Ref. [1] do we *explicitly* include a constraint on or promote sparsity. Specifically, our ℓ_1-norm cost function does not penalize spreading susceptance modification across the network as compared to concentrating the modification on a few lines. However, the sparsity of the solution emerges naturally.

One natural conjecture is that the l_1 norm in the cost function of Eq. (5) of [1] is the likely cause of sparsity, similar to the emergence of sparsity in compressed sensing, see e.g. [14]. However, there may be another, and equally plausible explanation, suggesting that the sparsity emerges from the "N-1 redundancy" engineered into electrical networks. Specifically, $N-1$ redundancy generally requires that there be at least two paths to deliver power to loads. If one of paths becomes overloaded, an increase in susceptance of an alternate path will deliver more power thus relieving the congestion on the first path. Alternatively, the susceptance of the overloaded path may be decreased pushing power flow onto the alternate paths. These arguments suggest an additional cutting plane-like heuristic that could speed up our algorithm even further: instead of optimizing over the susceptances of all of the lines, one could restrict the attention to the set of lines that are near to the overloaded lines.

III. Application to Realistic-Sized Cases: Polish Grid

The numerical experiments on the small 30-node test network in Section II built up some intuition about the properties of the solutions to optimal placement and sizing of SC devices. In this Section, we apply the algorithm of Ref. [1] to the example of the Polish grid—a realistically-sized network ($\sim$ 2700 buses) also available in MatPower[13]. In all of the case studies performed on the Polish grid, our algorithm converged in an unexpectedly small number of iterations – less than a dozen for all the cases we experimented on, with each iteration taking $\sim$30 seconds on a standard quad-core processor.

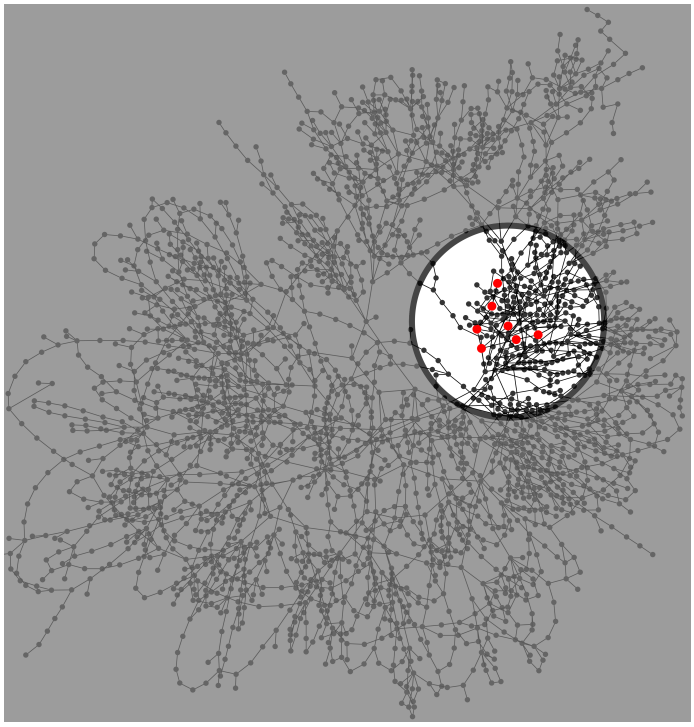

Fig. 3. Non-geographical visualization of the entire Polish grid. The highlighted region contains all of the overloaded and SC-modified lines for the cases shown in the table of Fig. 4. Part of the highlighted region is shown in more detail in Fig. 5 for $\alpha/\alpha_c = 1.38$ with the red nodes here corresponding to the large colored nodes of Fig. 5.

A. Stressing Via Uniform Load Growth

In this first study, we apply stress to the Polish grid using the same uniform load scaling as used in the 30-bus example.

rescaling	initially overheated lines	modified lines	
1.02	375	375	local
1.04	375	375	
1.1	375 2162	375	non-locality
1.24	375 2162	375	
1.29	375 2162 2585	315 375	
1.35	375 2162 2585	375 2156	
1.38	375 2162 2585	375 1976 2156	

Fig. 4. Table of (initially) overloaded lines and modified lines for the Polish grid in Fig. 3 for a few specific values of α/α_c. The modified lines are selected by our SC device placement algorithm [1]. The solution for $\alpha/\alpha_c = 1.38$ is shown in detail in Fig. 5.

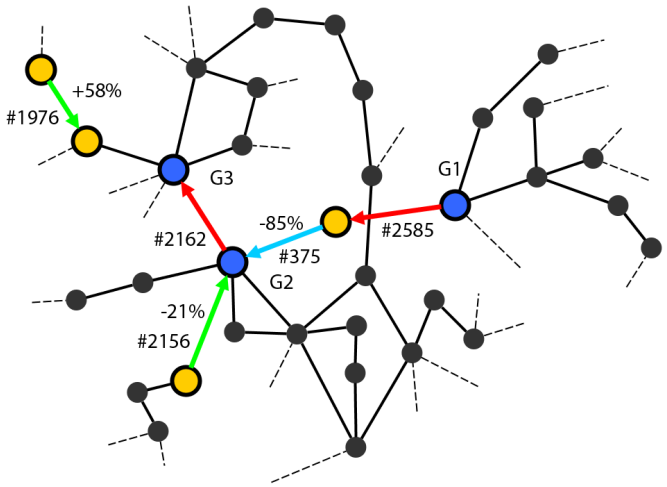

Fig. 5. Detail of the highlighted region of the Polish grid from Fig. 3 for $\alpha/\alpha_c = 1.38$. Generators nodes are blue and load nodes are yellow. The two red lines and one blue line were initially overloaded. The two green lines and one blue line are selected by our algorithm for susceptance modification. The arrowheads on the lines indicate the direction of power flow. The percentages next to the green and blue lines indicate the degree of susceptance modification.

We consider network stress up to $\alpha/\alpha_c = 1.38$. The results for several values of α/α_c are presented in the tabular form in Fig. 4. Figure 3 highlights the small region of the entire Polish grid where all of the overloads and susceptance modifications in from Fig. 4 occur.

The results in Fig. 4 demonstrate behavior qualitatively similar to the much smaller 30-bus network. For small α/α_c up to at least 1.04, the optimal solution is local, i.e. our algorithm chooses to relieve the single overloaded line (line 375) by simply reducing the susceptance of this line. As α/α_c grows, non-local behavior becomes apparent. For $\alpha/\alpha_c \geq 1.1$, additional lines become overloaded (lines 2162 and later 2585), however, none of these additional lines are selected for susceptance modification even though line 375 continues to be selected for susceptance modification in all of the solutions.

The details of the solution in the highlighted region of Fig. 3 are shown in Fig. 5 for $\alpha/\alpha_c = 1.38$. Before susceptance modification by the SC devices, the general arrangement of power flows results in power being sent from generator G1 towards generator G2 (on lines #2585 and #375) and subsequently to generator G3 (on line #2162) to feed loads beyond G3. It is these three lines which are overloaded at $\alpha/\alpha_c = 1.38$ before the correction by SC devices. In addition, power is brought towards generator G2 via line #2156. The corrections by the SC devices include a reduction in susceptance on line #375 to reduce the flow from G1 and relieve the overload of #375 and #2585. However, this is still not sufficient to relieve the overload of #2162. A decrease of susceptance of line #2156 and an increase on line #1976 decreases the bottom-to-top flow on #2162 to relieve its overload.

Fig. 6 displays the details of the solution and its evolution as a function of the network stress from α/α_c =1.0 to 1.38. The total cost of susceptance modification grows modestly from $\alpha/\alpha_c = 1$ to about 1.29. In this range, lines #375 and #2162 are overloaded in the base case. The steady reduction in the susceptance of line #375 begins the separation of generator G1 from G2 and G3, as discussed above for α/α_c =1.38. This reduction directly relieves the overload of #375 and indirectly relieves the overload of #2162. As α/α_c is increased beyond 1.29, the overloads on #375 and #2162 continue to increase but line #2585 that connects directly to generator G1 also overloads. The algorithm modestly lowers the susceptance of line #375 but the major change is to lower the susceptance of line #2156 to decrease the bottom-to-top flow on line #2162. Beyond α/α_c =1.35, even this is insufficient and the susceptance of line #1976 is raised to increase the top-to-bottom flow on that line (nominally toward G3) to help offset the flow into G3 on line #2162.

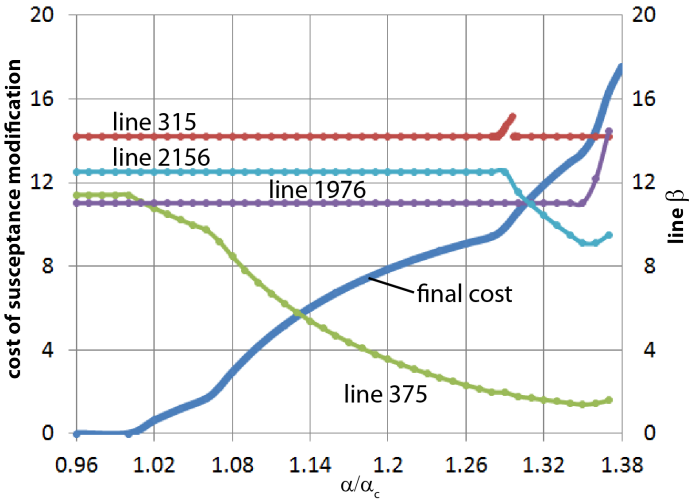

Fig. 6. Dependence of the optimal cost of susceptance modification (thick blue curve) and the modified susceptances (lines with filled circles) on the scaling factor α/α_c for the case study of the Polish grid in Fig. 4. Only lines which are modified are shown. Bends of the cost curve generally indicate the overload of an additional line.

B. Robust Optimal Placement and Sizing: Correcting Multiple Configurations

The example of uniform load scaling discussed above only considered one overload scenario at a time. As discussed in [1], we can also robustly optimize a *single* placement and sizing of SC devices to correct *multiple* overload scenarios — the overload scenarios are defined by their power injection vectors $p^{(1)}, \cdots p^{(i)}, \cdots p^{(n)}$ where n is the number of scenarios. The Sequential Linear Program (SLP) in Section IV-C of Ref. [1] is modified to include network constraints for each of the n overload scenarios. Then, on every iteration of the cutting plane step (see Fig. 1 of [1]), we find the $m^{(i)}$ transmission constraint inequalities to be "included" in the SLP for overload scenario i. We combine the list of inequalities across all n scenarios to create a single extended list of length $2m^{(1)} + \cdots 2m^{(i)} + \cdots 2m^{(n)}$. We then replace the list of the directed edge labels $\mathcal{E}^{(in)}$ in Eq. (7) of [1] with the new composite list and iterate the improved algorithm as described in Section IV-C of [1].

To demonstrate this method, we consider a simple situation where we robustly optimize the placement and sizing of SC devices against two overload scenarios. The first scenario is the Polish grid's winter off-peak configuration (from MatPower[13]). To generate a second scenario, we modify the same winter off-peak configuration. First, we non-uniformly scale the loads by multiplying each load by a scale factor X distributed between 0.3 and 1.7. The non-uniform load scaling is followed by a generation adjustment via solution of an optimal power flow. With our two scenarios of load and generation determined, they are both uniformly scaled (as done in the previous Subsection) to study the robust optimization results as a function of the system stress α/α_c.

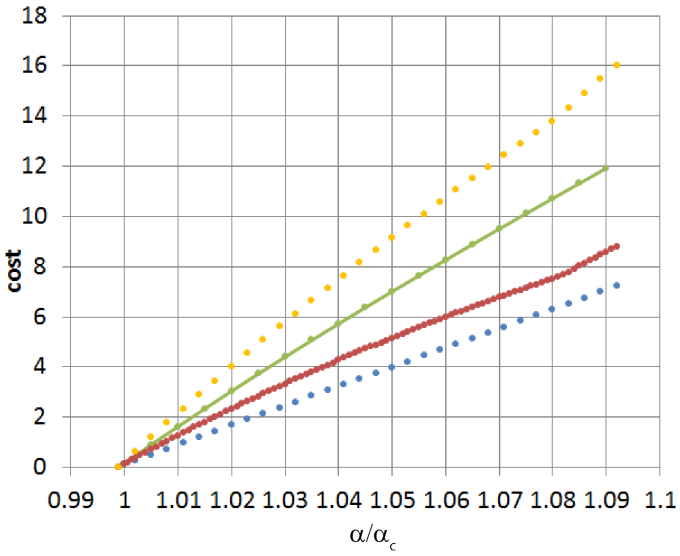

Fig. 7. Optimal cost vs α/α_c for the Polish grid: (red curve) optimization over the base, off-peak winter configuration, (blue curve) optimization over the non-uniformly scaled base case (see discussion in the text), (green curve) robust optimization over both the base case and the non-uniformly scaled base case. The yellow curve is the naive combination of the two independent optimizations, i.e. the sum of the maximum cost per line over both cases.

Fig. 7 shows the resulting cost of optimal SC susceptance modifications for the robust optimization (green curve) compared to the optimal SC susceptance modifications that independently consider one or the other scenario (red and blue curves). Since the robust optimization is jointly correcting both overload scenarios, the total cost is higher than either of the independent scenarios. However, it is lower than the yellow curve, which is the sum of the maximum cost per line in the two independent scenarios, i.e. the cost one would naively compute by optimizing SC placement and sizing for the two independent scenarios.

The cost advantage in the previous discussion stems from the robust formulation utilizing some of the SC devices to correct overloads in both scenarios. For this to occur the overloaded lines in the two scenarios must be in reasonable proximity to each other. If instead, the overloaded lines in the two scenarios are spatially well separated, the lack of interaction between the SC devices and transmission line constraints at these locations would effectively split the robust optimization back into two separate, independent optimizations. A second case where the robust optimization would not improve the results is when the scenarios have exactly the same set of line overloads. In the study presented in Fig. 7, we have purposely selected a randomly-generated second scenario that displays some overlap with the original, uniformly-scaled Polish winter base case.

C. Stressing Via Sequential Generator Retirement

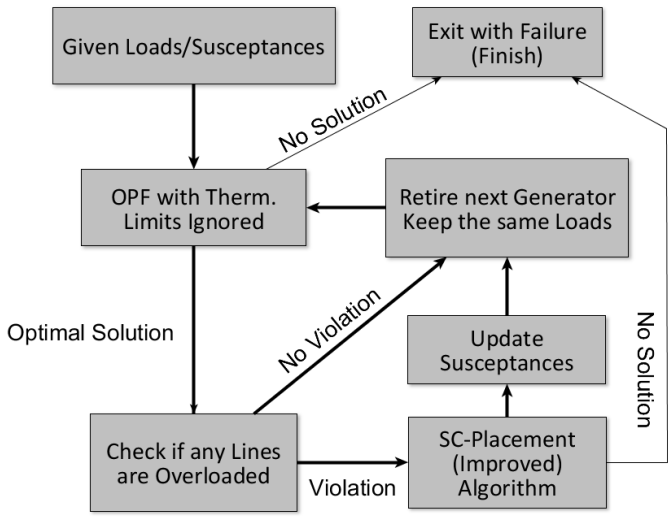

Fig. 8. Flowchart of the generation retirement process using the SC-device placement and sizing algorithm from Ref. [1]. The process can continue until one of two conditions apply: 1) the generator limits can no longer be met after retirement of a generator, or 2) the transmission line overloads can not be resolved by the SC-device placement and sizing algorithm. In principle, a new OPF could be solved to relieve the overload, but for simplicity, we terminate the process at this point.

Concerns about CO_2 emissions [15] [16] and the safety of nuclear plants [17] [18] [19], the imposition of renewable portfolio standards, and the low price of unconventional natural gas [20] have led to the retirement or planned retirement of many large coal and nuclear-fueled generators that have

provided inexpensive energy to grids in Germany and the United States, among others. The capacity lost via the retirements will eventually have to be replaced, typically by new natural gas-fired generation or renewable generation. If the retirements progress sequentially over time, this replacement may not be required immediately because the extra generation capacity in these systems may be sufficient to serve the loads with sufficient reserves. The retirement of each generator that supplies low-cost energy will lead to a new nominal ordering of generation units to provide the lowest-cost energy to the system. However, the configuration of power injections created by this new lowest-cost ordering may lead to new network violations requiring the output of the lower-cost generators to be reduced in favor of higher-cost units. Here, we seek to use SC devices relieve the network congestion to make the lowest-cost generation injections feasible.

We use the process outlined in Fig. 8 to apply our SC-device placement and sizing algorithm to the problem of sequential generator retirements. Starting with a fixed set of loads and network susceptances, we solve an OPF while ignoring transmission line thermal limits but still respecting generation limits. If this modified OPF is infeasible (due to generator limit violations), then new generation must be built to serve the existing load, and we exit. If this modified OPF is feasible, the solution is the lowest cost generation stack possible. Next, we check to see if the network power flows associated with the lowest-cost solution violates any transmission line limits. If not, we retire the next generator in the sequence and repeat the process. If there are line violations, we apply our SC-device placement and sizing algorithm from Part I of this work [1]. If the overloads can be resolved, we update the susceptances, retire the next generator in the sequence, and repeat the process. If the overloads cannot be resolved, we exit the process.

The algorithm of Fig. 8 was tested on the Polish grid (summer case) model with the results illustrated in Figs. 9-11. This case allowed the retirement of the four generators (red dots in Fig. 9) before becoming infeasible with respect to generation limits. The size of the red dot indicates the relative order of retirement, i.e. the generator with the largest dot was retired first. The order was determined by retiring the generator with the largest power output from the previous OPF in the process of Fig. 8. The retirement of these generators forces the others to increase their output to compensate (light blue dots in Fig. 8, and this response is widely distributed across the entire network. The resulting congestion is associated with the response of the two generators at either end of the red line in Fig. 9. This line is #2162 in in the detailed view of the congested region in Fig. 10.

As with the cases studied earlier, our SC placement and sizing algorithm makes both local and non-local changes to the line susceptances to correct the overloads. Specifically, the susceptance of line #375 is decreased (by $\sim$20%) while the susceptance of line #315 is increased (by $\sim$25%) to draw power flow toward line #315 to relieve the overloads on both lines #375 and #2162.

To measure the relative value of the SC-devices, we also solve an OPF with all the transmission line limits enforced and no SC-devices installed. The transmission congestion in this uncompensated system increases the total generation costs

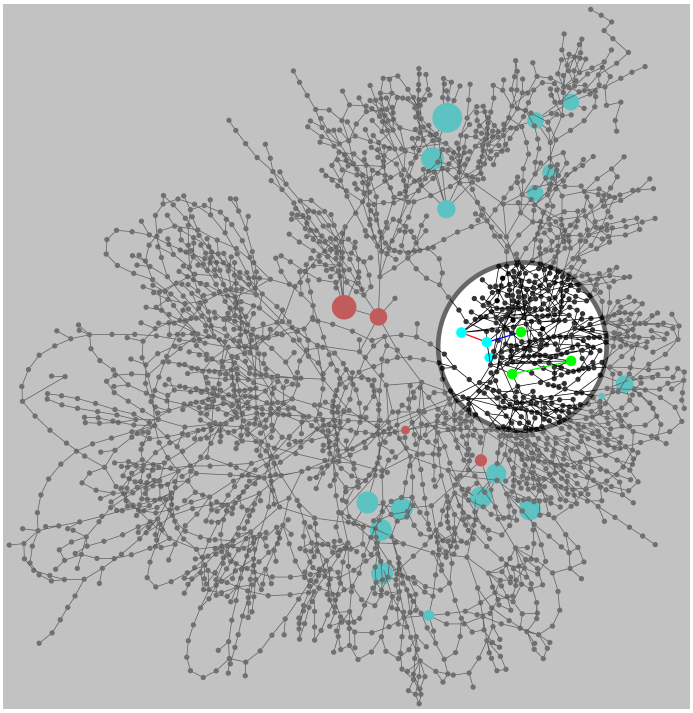

Fig. 9. Illustration of Polish grid used for the study of sequential generator retirement. The retired generators are marked with red dots with the dot size indicating order of retirement (from large to small). The blue dots mark the generators whose output is increased by the optimal power flow with the size of the dot indicating the magnitude of the power output increase. All line overloads and susceptance corrections occur in the highlighted region. The red line is overloaded. The blue line is overloaded and has its susceptance modified. The green line only has its susceptance modified. The green dots in the highlighted region only serve to highlight the colored lines. A detail of the highlighted region is shown in Fig. 10.

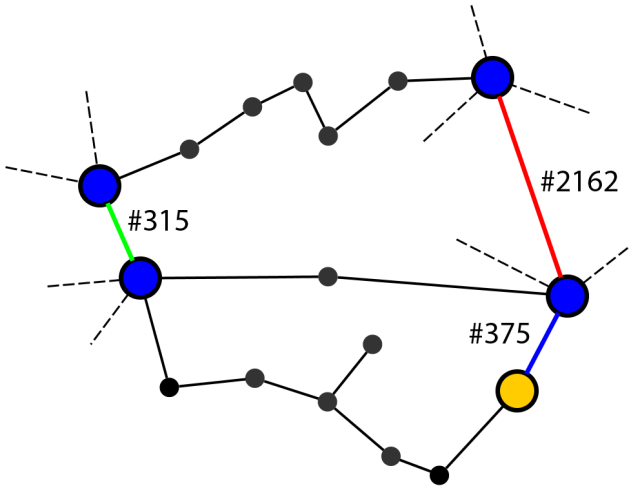

Fig. 10. Cropped portion of Fig. 10 magnifying the region of the grid where all overloaded and corrected lines are located. Blue nodes are generators and yellow nodes are loads. The generators that respond to the retirements by increasing their outputs are at either end of line #2162. The transmission line color coding is the same as in Fig. 9.

over the system that uses SC-modified line susceptances. Fig. 11 compares the cost of generation in these two systems. As expected, the cost of generation grows as the low-cost generation is removed via retirement. After the fourth stage of retirement, the system with optimal SC-device placement shows cost ∼$1.0K/hour lower than the system without SC-devices. Over the entire year, this difference amounts to approximately $9M, however, the congestion is not likely to be present all hours of the year and the estimated annual savings should be weighted by the fraction of the time the congestion appears.

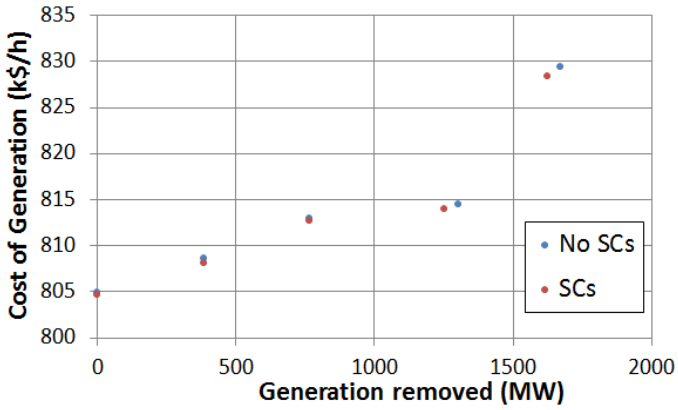

Fig. 11. Total cost of generation versus the amount of generation retired for the Polish network of Fig. 9. The blue circles indicate the cost for case when the network congestion is relieved by redispatching generation via an optimal power flow. The red circles are the cost for the case when then congestion is relieved by SC-devices using the algorithm of Ref. [1]. The amount of generation measured by the amount of power supplied by the generator on the last iteration, not by the capacity. This results in small differences in the generation removed in the two cases.

IV. Conclusions

In a companion manuscript [1], we developed an algorithm for placement and sizing of series compensation (SC) devices over a large networks. In this manuscript, we have applied this algorithm to a range of cases to demonstrate its computational efficiency and to illustrate the effect and utility of SC devices in relieving network congestion. The computational efficiency arises from an underlying sparsity in the problem (which we conjecture is due of our use of the ℓ-1 norm) and our exploitation of that sparsity using cutting plane methods. The computational efficiency enables the resolution of congestion in realistic-sized networks (∼2700 nodes and ∼3300 lines) in tens of seconds. We have demonstrated that a slightly modified robust version of our algorithm can resolve multiple configurations of network congestion with a single placement of SC devices. We find that if the congestion in the configurations are in reasonable proximity, the robust solution may have lower cost solutions than if the individual cases of congestion are resolved individually. Finally, we have applied our algorithm to a problem of sequential retirement of low-cost generators. We showed that a few SC devices can resolve network congestion associated with these retirements and enable the remaining low-cost generation to be maximally utilized.

Extensions of this work and that in Ref. [1] may include:

- Resolution of congestion due to exceeding voltage limits and/or dynamic stability thresholds
- Inclusion of a broader range of FACTS beyond SC devices and the consideration of the effects of other technologies such as energy storage
- Reformulation of the algorithm to enable the robust, low-cost placement of SC devices (or the other mentioned above) over a time horizon to resolve network congestion that appears because of a predicted time sequence of events.

The work at LANL was carried out under the auspices of the National Nuclear Security Administration of the U.S. Department of Energy at Los Alamos National Laboratory under Contract No. DE-AC52-06NA25396. This material is based upon work partially supported by the National Science Foundation award # 1128501, EECS Collaborative Research "Power Grid Spectroscopy" under NMC. The work of VF was partially supported by the Ministry of Education and Science of Russian Federation.

References

[1] V. Frolov, S. Backhaus, and M. Chertkov, "Efficient algorithm for locating and sizing series compensation devices in large transmission grids: Model implementation," 2013.
[2] M. Noroozian, L. Angquist, M. Ghandhari, and G. Andersson, "Use of upfc for optimal power flow control," *Power Delivery, IEEE Transactions on*, vol. 12, no. 4, pp. 1629 –1634, oct 1997.
[3] A. Del Rosso, C. Canizares, and V. Dona, "A study of tcsc controller design for power system stability improvement," *Power Systems, IEEE Transactions on*, vol. 18, no. 4, pp. 1487–1496, 2003.
[4] A. Sode-Yome, N. Mithulananthan, and K. Lee, "A comprehensive comparison of facts devices for enhancing static voltage stability," in *Power Engineering Society General Meeting, 2007. IEEE*, 2007, pp. 1–8.
[5] J. V. Milanovic, "Modeling of facts devices for voltage sag mitigation-studies in large power systems," *IEEE TRANSACTIONS ON POWER DELIVERY*, vol. 25, no. 4, 2010.
[6] H. F. Wang, H. Li, and H. Chen, "Coordinated secondary voltage control to eliminate voltage violations in power system contingencies," *Power Systems, IEEE Transactions on*, vol. 18, no. 2, pp. 588–595, 2003.
[7] P. Albrecht and G. Breuer, *Flexible ac transmission systems (FACTS): scoping study*, ser. Flexible Ac Transmission Systems (FACTS): Scoping Study. General Electric Company. Power Systems Engineering Dept and Electric Power Research Institute, 1991, no. v. 2, pt. 1. [Online]. Available: http://books.google.com/books?id=UPwJAQAAMAAJ
[8] "Flexible ac transmission systems (facts)," http://en.wikipedia.org/wiki/Flexible_AC_transmission_system.
[9] "Proposed terms and definitions for flexible ac transmission system (facts)," *Power Delivery, IEEE Transactions on*, vol. 12, no. 4, pp. 1848 –1853, oct 1997.
[10] N. Hingorani and L. Gyugyi, *Understanding FACTS: Concepts and Technology of Flexible AC Transmission Systems*. Wiley-IEEE Press, 1999.
[11] ——, *Understanding FACTS concepts and technology of flexible AC transmission systems*. IEEE Press, New York, 2000.
[12] R. Mathur and R. Varma, *Thyristor-based FACTS controllers for electrical transmission systems*. IEEE Press, Piscataway, 2002.
[13] [Online]. Available: http://www.pserc.cornell.edu/matpower/
[14] E. J. Candes, M. B. Wakin, and S. Boyd, "Enhancing sparsity by reweighted l1 minimization," *Journal of Fourier Analysis and Applications*, vol. 14, no. 5, pp. 877–905, 2008.
[15] C. Butcher, "Europe: More coal, then less," *Power Magazine*, 2012.
[16] L. Fleischman, R. Cleetus, J. Deyette, S. Clemmer, and S. Frenkel, "Ripe for retirement: An economic analysis of the u.s. coal fleet," *The Electricity Journal*, vol. 26, pp. 51–63, 2013.

[17] "Decommissioning nuclear facilities," http://www.world-nuclear.org/info/Nuclear-Fuel-Cycle/Nuclear-Wastes/Decommissioning-Nuclear-Facilities/, 2013.
[18] "Nuclear power in germany," http://www.world-nuclear.org/info/Country-Profiles/Countries-G-N/Germany/, 2013.
[19] J. Johnson, "Nuclear retirement anxiety," *Chemical & Engineering News*, vol. 91, pp. 14–17, 2013.
[20] M. Ratner and M. Tiemann, "An overview of unconventional oil and natural gas: Resources and federal actions," https://www.fas.org/sgp/crs/misc/R43148.pdf, 2013.